European Journal of Medicinal Chemistry 215 (2021) 113289

Contents lists available at ScienceDirect

European Journal of Medicinal Chemistry

journal homepage: http://www.elsevier.com/locate/ejmech

Research paper

The total synthesis of berberine and selected analogues, and their evaluation as amyloid beta aggregation inhibitors

Misato Tajiri, Ryo Yamada, Mayumi Hotsumi, Koki Makabe, Hiroyuki Konno*

Graduate School of Science and Engineering, Yamagata University, Yonezawa, Yamagata 992-8510, Japan

ARTICLE INFO

Article history:
Received 27 December 2020
Received in revised form
5 February 2021
Accepted 9 February 2021
Available online 13 February 2021

Keywords:
Berberine
Alzheimer's disease
Amyloid beta
Aggregation inhibition

ABSTRACT

The total synthesis of berberine and selected analogues. And their evaluation as amyloid β (Aβ) aggregation inhibitors is described. The key step in the synthesis, the assembly of the berberine framework, was accomplished using an intermolecular Heck reaction. Berberine analog **17** incorporating a tertiary amine moiety showed good anti Aβ aggregation activity, water solubility, and almost no toxicity to nerve cells.

1. Introduction

Amyloid β (Aβ) is peptide consisting of 36–43 amino acid residues generated from amyloid β precursor protein (APP) [1]. It is potently neurotoxic, rapidly forming aggregates such as soluble oligomers and protofibrils; and insoluble amyloid fibrils with a β-sheet structure which kill nerve cells and are believed to be the cause of Alzheimer's disease (AD) [2]. The inhibition of Aβ aggregation has therefore been suggested as an effective strategy for AD therapeutic drug development, and several studied concluded the herbal supplement curcumin, to impart anti-AD activity [3–6]. However, a clinical trial of curcumin for the treatment of AD patients ended in failure [7], perhaps due to its poor water solubility [8]. Accordingly, curcumin analogues exhibiting improved absorption and pharmacokinetics is needed. Previously, we demonstrated that the Aβ aggregation inhibitory activity and water solubility of curcumin could be dramatically improved by addition of an appropriately-located phenolic hydroxyl group [9–13], but the resulting analogues were too metabolically unstable and inadequately soluble for their future development as therapeutic drugs. Accordingly, we re-focused our efforts on alkaloids such as galanthamine [14], which were recently shown to inhibit Aβ aggregation; and 9-methylfascaplysin [15], which recently served as a lead compound substitute for curcumin.

Berberine (**1**) is a benzyl isoquinoline alkaloid contained in *Coptis Japonica*, a herb whose extracts have long been used as an antidiarrheal and eye drop. More recently, berberine (**1**) has been demonstrated to impart various physiological activities, such as anti-inflammtory [16], antibacterial [17], and neuroprotective effect [18], and there has been growing interest in its application as a treatment for central nervous system diseases [19]. Structurally, berberine (**1**) corporates four consecutive rings, which are considered to be more stable in the body than curcumin and its analogues; and its methylene acetal group can be regarded as a latent phenolic hydroxy group – the deprotection of which is anticipated to improve its Aβ aggregation inhibitory activity (vide infra).

Prior to initiation of a structure activity relationship study of berberine (**1**) analogues, we undertook the total synthesis of berberine (**1**) for the purpose of determining the partial structure required for Aβ aggregation inhibitory activity. Several syntheses of berberine (**1**) have been reported, but they are neither amenable to the synthesis of analogues, nor practical scale-up, in part due to a reliance on expensive catalysts or starting materials [20–22]. In the present study, we report a novel total synthesis of berberine (**1**) and its analogues, and the evaluation of their Aβ aggregation inhibitory activity, and selected pharmacokinetic and physical properties.

2. Result and discussion

Synthesis of berberine (1) and its analogues (12)–(17).

* Corresponding author..
E-mail address: konno@yz.yamagata-u.ac.jp (H. Konno).

https://doi.org/10.1016/j.ejmech.2021.113289
0223-5234/

Our synthetic strategy is outlined in Scheme 1. The key step for construction of the berberine framework (**2**) is an intramolecular Heck reaction of the *N*-alkylation product of isoquinoline (**4**) and alkyl bromide (**5**) (Scheme 1).

First, we synthesized isoquinoline **4** (Scheme 2). Jones oxidation of 2,3-dimethoxybenzaldehyde **6** gave carboxylic acid **7** in a yield of 80%. After converting **7** to the acid chloride, coupling with amino acetaldehyde diethyl acetal gave amide **8** in 83% yield over two steps. Treatment of **8** with conc. H_2SO_4 from 0 °C to room temperature over 72 h (the Pomeranz Fritsch isoquinoline synthesis) gave isoquinoline **4** in 77% yield [23,24] (Scheme 2).

Alkyl bromide **5** was obtained from piperonal **9**. Wittig reaction of **9** followed by hydrolysis with 2 M HCl aqueous solution gave aldehyde **10**, which was subsequently reduced with $NaBH_4$ to give alcohol **11** in 97% yield. Bromination of **11** using NBS, followed by the bromination of the primary hydroxyl group (the Appel reaction) gave alkyl bromide **5**. Next, the *N*-Alkylation of **4** with **5** was attempted. No desired compound **3** was obtained using strong bases (NaHMDS or NaH) -elimination of the bromide of **5** occurred instead. Use of weak bases ($NaHCO_3$ or K_2CO_3), effectively suppressed this elimination, but very little of the desired *N*-alkylation product was isolated. Eventually, we found that use of the highly soluble, weak base Ce_2CO_3 in DMF at 80 °C gave the desired product **3** in 32% yield after an extended reaction time [24]. With **3** in hand, we sought to assemble the berberine framework (**2**) with a Heck reaction. Using catalytic amount of $Pd(OAc)_2$/DIPEA/PPh_3 in toluene, desired product **2** was obtained in 25% yield. The reaction was monitored by ^{1}H NMR – the proton peak corresponding to the double bond of **3** [6.25 ppm (d, J = 7.6 Hz, 1H)] was observed to disappear. Finally, reduction reaction of **2** with $LiAlH_4$ in refluxing THF gave berberine (**1**) in 16% yield. The ^{1}H NMR spectra of our synthetic berberine (**1**) was consistent with that reported in the literature [23], including with the peaks at 9.87 ppm, s, 1H and 8.91 ppm, s, 1H that are indicative of the isoquinoline framework. Thus, the total synthesis of berberine (**1**) was achieved in 8 steps from compounds **9** and **4** (Scheme 3).

A selection of berberine analogues all bearing varying numbers of phenolic hydroxyl groups was also prepared from berberine (**1**) by deprotection of the methoxy groups and methylene acetal. Analogues **12**–**14** were obtained by adjusting the reaction time, and the amount of BBr_3 used. In order to investigate the effect of the oxidation state, charge, and geometry of the nitrogen center on the physical properties of the analogues, berberine (**1**) was reduced with $NaBH_4$ to obtain quinolizidine **15** in 83% yield. Treatment of quinolizidine **15** with BBr_3 in CH_2Cl_2 gave triol **16** and tetraol **17** in yields of 44% and 28%, respectively. **15**, **16** and **17** as a racemate were used for following assays (Scheme 4) (see Fig. 1).

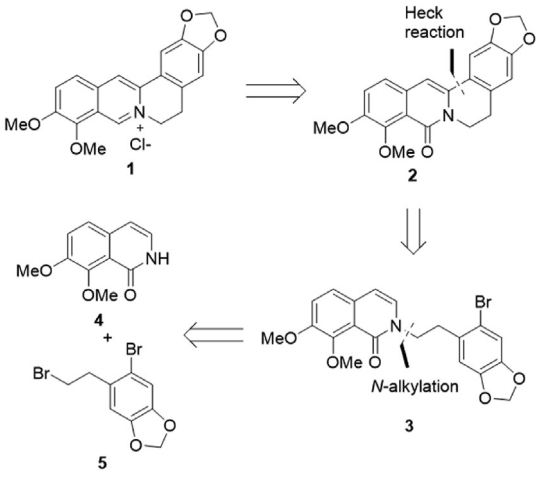

Scheme 1. Retrosynthetic analysis of berberine (**1**).

2.1. Anti aβ aggregation assay

The anti Aβ aggregation activity of our berberine analogues was investigated by the widely-used thioflavin T (ThT) method [25,26]. Fresh Aβ42 (25 μM) was incubated at 37 °C with ThT and the fluorescence of the mixture measured every hour for 0–20 h. The fluorescence was found to follow a sigmoidal-like curve, with a point of inflection. There was an initial lag time of about 2 h (corresponding to the aggregation of monomeric Aβ42 to oligomer and/or protofibrils), the fluorescence sharply increased at about 4–6 h (corresponding to the aggregation of protofibrils to amyloid fibrils) (Fig. 2). The extent of Aβ42 aggregation after 20 h was defined to be 100% (= control). Incubation of a mixture of 25 μM monomeric Aβ42 and 10 μM berberine (**1**) at 37 °C resulted in a similar sigmoidal-like curve with a final equilibrium level of 68%. Thus, berberine (**1**) at a concentration of 10 μM was found to inhibit Aβ aggregation (25 μM) at a ratio of 32%. On the other hand, the inhibition rate of intermediates **2**–**4**, **8** was negative (Table 1). (i.e. the addition of the **2**–**4**, and **8** increased the intensity of the fluorescence), indicated that these intermediates did not inhibit any Aβ aggregation. Although it is still possible that **2**–**4** and **8** bind to Aβ fibrils, these compounds do not show fluorescence (data not shown). Based on these results, we concluded that the berberine framework is essential to anti Aβ aggregation, although the activity of berberine (**1**) was less than of curcumin (10 μM, 80%) and some of the curcumin analogues (10 μM, 100% for AY1319 and AY1511). Trends noted from the contrasting inhibition rates of the analogues tested show that inhibitory activity increases in proportion to the number of phenolic hydroxy groups, and that structures incorporating a tertiary amine (**16**–**17**) showed higher activity than those incorporating quaternary ammonium salts (**12**–**14**) (Table 1). Tetrahydroxy quaternary amine **14** and tetrahydroxy tertiary amine **17** showed the inhibition of the formation of Aβ fibril with 72% and 78%, respectively (Fig. 2A).

2.2. DLS measurements

The morphological change of Aβ species caused by the addition of berberine analogues to their solutions was also assessed, using dynamic light scattering (DLS) [27,28]. Tertiary amine **17** was selected for this study, having good water solubility. Based on the DLS results, we estimate that the Aβ monomer formed an aggregate with a diameter of about 4.6 μm after 20 h of incubation. On the other hand, the diameter of the Aβ aggregate in the presence of **17** was 1.3 nm. Therefore, **17** was concluded to potently inhibit the aggregation of Aβ such that it forms oligomers and/or nano-rod like structures only (Fig. 2B).

2.3. Cytotoxicity

The cytotoxicity of the berberine intermediates and analogues toward highly differentiated rat pheochromocytoma (PC-12) cells was evaluated in a standard water-soluble tetrazolium-8 (WST-8) assay [29–31]. PC-12 cells were cultured in a medium of Dulbecco's modified eagle medium (DMEM) with 10% fetal bovine serum at 37 °C in an atmosphere of 5% CO_2. For WST-8 assays, the PC-12 cells were plated in 96-well plates at a density of 1.0×10^4 cells per well for 24 h. Then the compounds added to the well plates (as solution in 1% DMSO) and co-cultured for 24 h. PC-12 cells were treated with

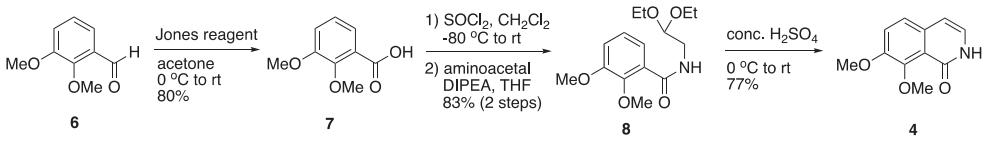

Scheme 2. Preparation of isoquinoline (**4**).

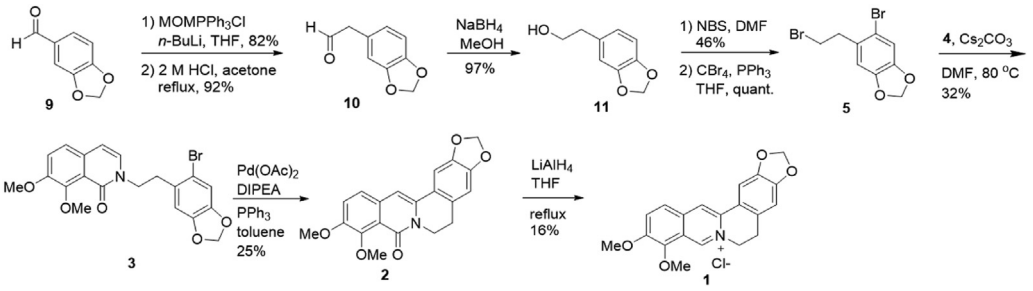

Scheme 3. Synthesis of berberine (**1**).

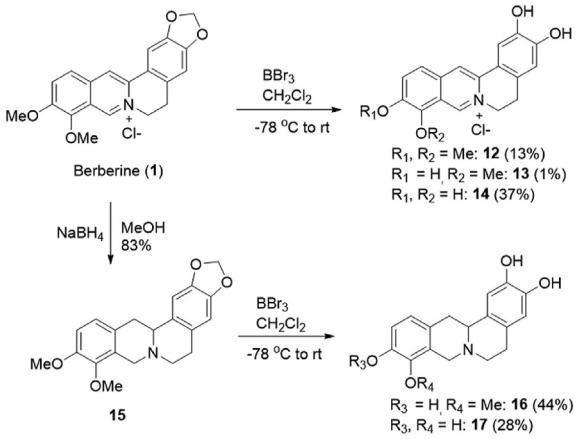

Scheme 4. Synthesis of berberine analogues (**12**–**17**).

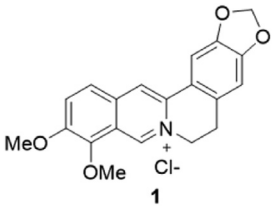

Fig. 1. Berberine (**1**).

WST-8 for 3 h at 37 °C. The generated formazan was detected by measuring the absorbance of the reaction mixture at 450 nm. The cytotoxicity of curcumin was also assessed as the control (CC_{50} = 44 μM). Berberine (**1**) and its synthetic intermediates **2**–**4**, **8**, synthetic analogues **12** and **15** showed almost no cytotoxicity (CC_{50} > 100 μM). The cytotoxicities of methoxy derivatives **13** and **16** were also lower than curcumin. In comparison, tetrahydroxy quaternary amine **14** (CC_{50} = 9.8 μM) exhibited moderate cytotoxicity against PC12 cells, and the cytotoxicity of tetrahydroxy tertiary amine **17** (CC_{50} = 114 μM) was significantly lower than that of curcumin (Table 1) (Fig. 2C).

2.4. Water solubility test [32]

The poor water solubility of curcumin has prevented its therapeutic development [8], and it was hoped that the water solubility of berberine (**1**) would be improved in comparison. Accordingly, UV–vis and HPLC analysis were conducted to evaluate the water solubility of berberine (**1**) and its analogues. Identical molar quantities each compound (**2**–**4**, **8**, **12**–**17**) were vortexed in water, and the resulting solutions centrifuged to remove undissolved material. The supernatant liquid was concentrated and the residue dissolved in MeOH or DMSO for analysis by RP-HPLC. The results are summarized in Table 1 and Fig. 2C. The water solubility of berberine (**1**) was 1874 μM, 9000 times higher than that of curcumin. The water solubility of **15** was much lower than berberine (**1**). However, those berberine analogues bearing two or more phenolic hydroxyl groups showed water solubilities equal to or higher than that of berberine (**1**). The tertiary amine analogues (**16**–**17**) were more water-soluble than the quaternary ammonium salt analogues (**12**–**14**), which had a hydroxyl group at the same position. In conclusion, incorporation of the catechol and tertiary amine moieties together improved water solubility (Table 1). Tetrahydroxy tertiary amine **17** was particularly water soluble (>3343 μM) (Fig. 2D).

2.5. Measurements of tPSA and ClogP

The topological polar surface area (tPSA) of a molecule is commonly used to assess and optimize its ability to permeate the blood-brain barrier. In generally, a tPSA of fewer than 90 Å squared is needed for a molecule to be considered as a lead compound [33,34]. The ClogP is also an important parameter [35] – a reasonable ClogP being no greater than 5.0. As shown in Table 1, curcumin and its analogues AY1319 and AY1511 showed tPSA values of 96.22, 97.99 and 107.22 Å – too high to be developed further. In contrast, berberine (**1**), its synthesized intermediates (**2**–**8**), and its analogues (**12**–**17**) all have tPSA values lower than the 90 Å squared threshold. The ClogP for all compounds was under 5.0. Therefore, all of these berberine-related compounds are suitable for further development as Aβ aggregation inhibitors (Table 1).

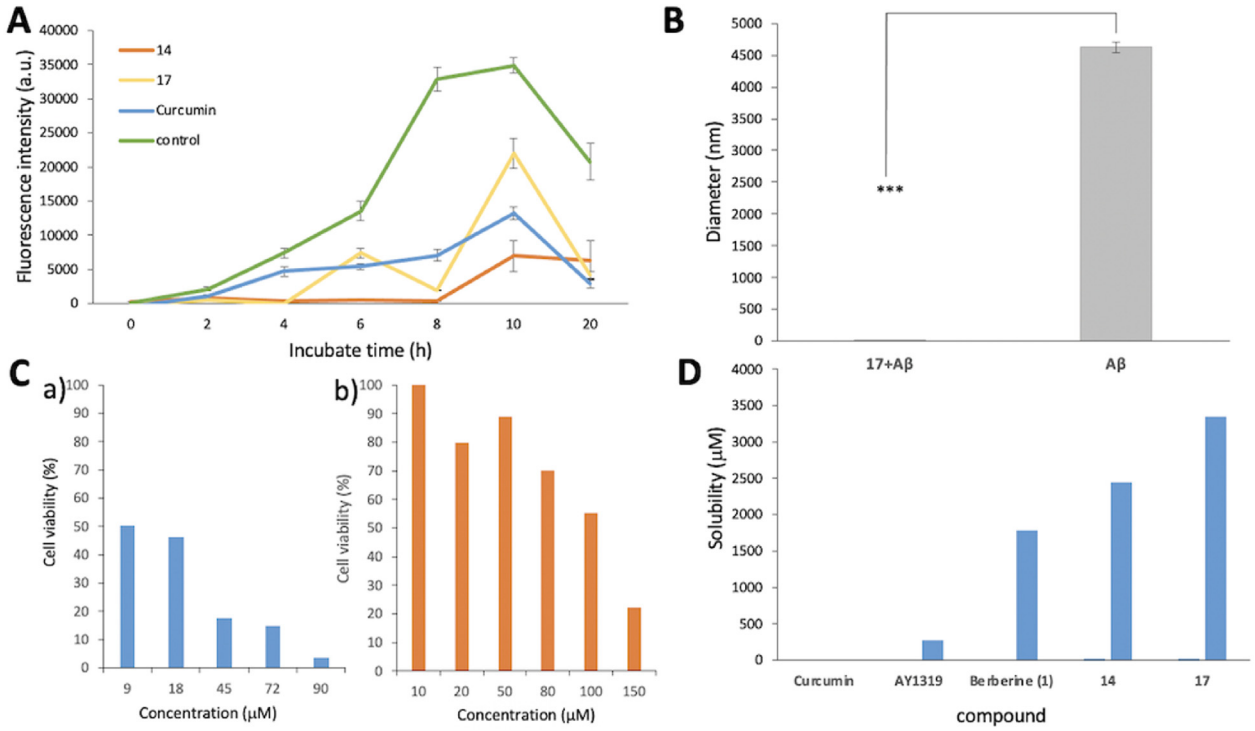

Fig. 2. (**A**) Time course of anti Aβ aggregation inhibition of curcumin and **14**, **17**. Values and error bars correspond to the average and standard deviation of three measurements, *p < 0.05 versus control. (**B**) Determination of the size of Aβ oligomers after 20 h incubation using DLS. Values and error bars correspond to the average and standard deviation of three measurements, ***p < 0.05. (**C**) Cell viability of the PC12 cell lines after addition of **14** (a) and **17** (b). (**D**) Comparison of water solubility of curcumin, AY1319, berberine (**1**) and its analogues (**14**, **17**).

Table 1
The anti Aβ aggregation activity, water solubility, cytotoxicity of synthesized berberine (**1**), synthetic intermediates (**2**–**4**, **8**) and its analogues (**12**–**17**).

entry	compound	aggregation inhibition[a] (%)	solubility[b] (μM)	cytotoxicity CC_{50} (μM)	tPSA	ClogP
1	Curcumin	80	0.19	44	96.22	2.17
2	AY1319	100	271	59	97.99	2.46
3	AY1511	100	2339	114	107.22	1.50
4	berberine (**1**)	32	1784	>150	28.53	3.17
5	**2**	−79	–	137	57.23	2.72
6	**3**	−63	15	132	57.23	3.89
7	**4**	−34	5.2	129	47.56	1.03
8	**8**	−49	26	>150	66.02	1.73
9	**12**	27	2753	>150	28.53	2.61
10	**13**	39	1496	39	50.09	2.35
11	**14**	72	2450[c]	9.8	62.04	2.09
12	**15**	−28	7.0[c]	>150	74.95	3.17
13	**16**	61	2372	91	65.06	2.35
14	**17**	78	>3343	114	77.98	2.09

[a] Aggregation inhibition values of Aβ after a 20 h incubation at 25 μM were indicated using 10 μM (except **1**, **12**–**14**) or 9 μM (**1**, **12**–**14**) inhibitors and calculated based on the ThT-based fluorescence spectroscopy assay (excitation = 440 nm, emission = 490 nm).
[b] Water solubilities were measured by the Dolai's protocol to show the values with μM.
[c] DMSO was used instead of MeOH.

2.6. TEM images

Transmission electron microscope (TEM) studies were undertaken, to visualize the morphology of the Aβ aggregation and its inhibition by berberine analogues [36]. In the absence of any aggregation inhibitor, mature Aβ fibrils with a length of 1 μm or more could be readily discerned (Fig. 3A). However, incubation of Aβ with **14** or **17** these fibrils transformed them into small and thin fragments of roughly 50 nm in size (Fig. 3B and C). The size of the fibrils formed from a mixture of **17** + Aβ as measured by DLS (Fig. 2B) and TEM (Fig. 3B and C) were identical suggesting that the tertiary amine **17** and quaternary ammonium salt **14** bind to Aβ protofibrils and inhibit the growth into higher aggregates and gave the oligomers and/or nano-rod like structures (Fig. 3A–C).

2.7. CD spectra

CD spectra were next acquired, to assess the concentration of β-sheet structure present in the solutions of Aβ. Solutions of the oligomers and/or these nano rod-like fragments exhibited reduced fluorescence intensity, compared to that with the fibrils – a finding attributed to the destruction of these high-ordered structures upon the binding of **14** or **17**. A decrease in the extent of β-sheet structure was inferred from the CD spectra, suggesting that Aβ aggregation

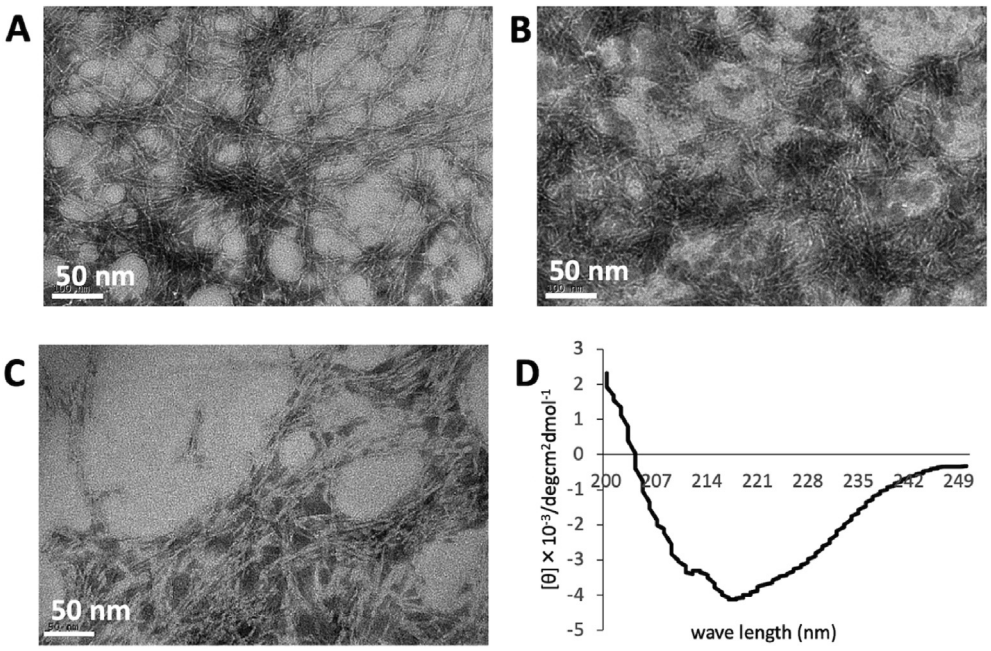

Fig. 3. Negative-staining TEM images and CD spectra of Aβ aggregation after 20 h incubation. (**A**) Aβ aggregation with ThT. (**B**) With **14**. (**C**) With **17**. Scale bars = 50 or 100 nm. (**D**) CD spectrum of Aβ nano rod-like structure with **17**.

was not eliminated, but merely that the resulting structures more closely resembled nano-rods than fibrils (Fig. 3D). These nano-rod-like fragments are known to be less cytotoxic than amyloidogenic Aβ intermediates, protofibrils and amyloid fibrils, and much more susceptible to cellular internalization. Notably, the cytotoxicity assay (Fig. 2) determined that the formation of oligomers and/or nano rods constructed from 10 or fewer Aβ units were insufficient to cause cell death; and their colocalization with lysosomal enzymes *in vitro* suggests their digestion to be efficient [37].

2.8. Docking simulation

Having established that the berberine analogues could effectively bind to the Aβ fibrils and disrupt their aggregation, a molecular docking analysis was performed to better understand this process. GOLD software [38] (Cambridge Crystallographic Center) was used to simulate the docking mode of **14** and **17** on a 12-fold Aβ(11–42) fibril structure (PDBID:2MXU). It was found that as **14** approaches the hydrophilic part of Aβ, the three phenolic hydroxyl groups form hydrogen bonds with ^{19}Phe, ^{22}Glu (Fig. 4A). The two hydroxy groups of the 3,4-cathechol ring of **14** interact with the amide carboxyl group of ^{19}Phe, and the hydroxy group of the isoquinoline ring of **14** interacts with the carboxylic acid group of the side chain of the ^{22}Glu of the Aβ fibrils (Fig. 4B). The docking of curcumin analogues AY1511 and AY1319 was also studied – their phenolic hydroxy groups and/or ketone carbonyl group were also found to interact with the amide carboxyl group of ^{19}Phe and the carboxylic acid group of side chain of the ^{22}Glu of the Aβ fibrils. These results have good similarity although are somewhat speculative due to the *in silico* nature of the study. However, binding to the hydrophilic part of the Aβ fibrils, especially the ^{16}Lys- [17]Leu- [18]Val- [19]Phe- [20]Phe sequence considered to be a nucleus for aggregation, is a characteristic of the binding mode found in curcumin and its analogues with high anti Aβ aggregation activity [9], and consistent with the docking results. On the other hand, the simulation also suggested that **17** binds to the Aβ hydrophilic part (^{18}Val, ^{19}Phe, ^{22}Glu) and **14** also binds to the hydrophobic part (^{32}Ile, ^{33}Gly, ^{34}Leu) (Fig. 4C). The binding mode of **17** with the Aβ hydrophilic part is similar that noted for **14** including the hydrogen bonding networks (data not shown). However, the binding of the phenolic hydroxy groups of **17** to the amide carbonyl groups of ^{33}Gly of Aβ fibrils was also predicted by the simulation (Fig. 4D). In our previous reports, we noted that the hydrophobic moiety of the Aβ fibrils interacts strongly with the hydrophobic methyl curcumin and ThT, causing them to be fluorescent [11]. Additionally, these interactions do not result in the collapse of the Aβ fibrils, or and inhibit the formation of additional Aβ fibrils. Thus, **17** binds to the Aβ hydrophilic part of Aβ less strongly than curcumin analogues AY1511 and AY1319, which presumably accounts for the lower aggregation inhibitory activity of **17** compared to the curcumin analogues. Moreover, the approach to the sequence of ^{32}Ile- [33]Gly- [34]Leu, the Aβ hydrophilic part, is a common feature with ThT, but its binding mode is considered to be different.

2.9. Calculation of stable conformation

To further investigate their effect on Aβ aggregation, the stable conformations of bound tertiary amine (**17**) and quaternary ammonium salt (**14**) were calculated by SPARTAN′19;[39] the results are shown in Fig. 5. Quaternary ammonium salt (**14**) was found to adopt four conformations (Energy: 222.79, 231.57, 238.38 and 273.04 kJ/mol), the most stable of which incorporated as a small twist. Thus, the flexibility of the frameworks of **12**–**14** is restricted by the quaternary nitrogen. On the other hand, 17 conformations were predicted for the tertiary amine compound (**17**), and the most stable of which was twisted more than any of those for quaternary ammonium salt (**14**). In the most stable conformations of **14** and **17**, the dihedral angle between the two surfaces sandwiching the C ring was calculated to be 21.55° for **14** (Figs. 5A) and 55.30° for **17** (Fig. 5B). Three of the 17 conformations calculated for **17** were selected for study by density functional theory (DFT) calculations. Their energies were calculated to be −2661399.24, −2661398.88, and −2661391.26 (a.u.) and the dihedral angle 55.30°, and are therefore believe to represent the

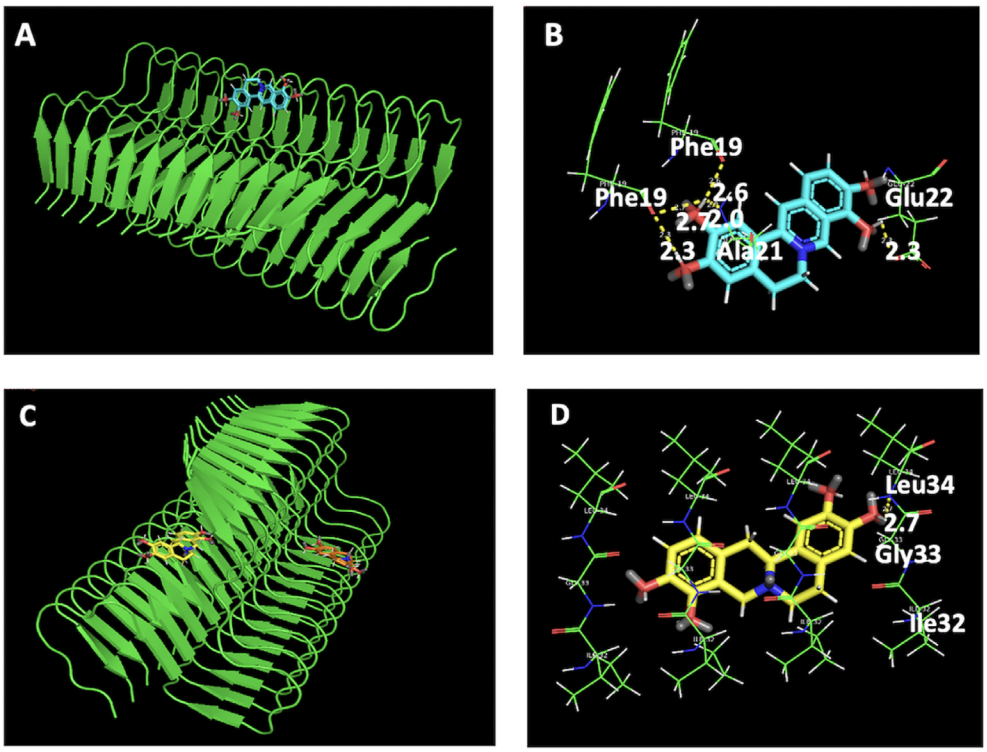

Fig. 4. (a) Binding pose of **14** in the Aβ fibrils; (b) Detailed view of docked **14** structure and the interacting amino acid moieties within the binding site of Aβ fibrils; (c) Binding pose of **17** in the Aβ fibrils; (d) Detailed view of docked **17** structure and the interacting amino acid moieties within the binding site of and (d) hydrophobic part of Aβ.

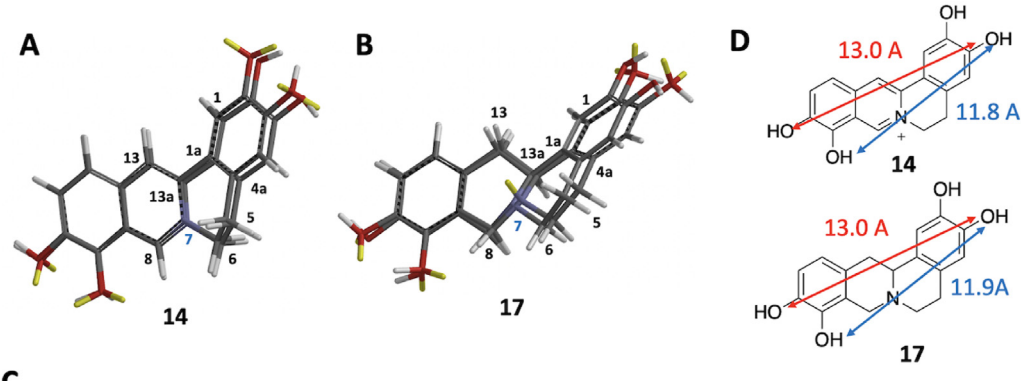

C

	14		17	
	closest	most stable	closest	most stable
a° ($_{13}$C-$_{13a}$C-$_{1a}$C-$_{1}$C)	21.55	21.55	49.04	49.12
b° ($_{13}$C-$_{13a}$C-$_{7}$N-$_{8}$C)	1.47	1.47	68.00	68.09
c° ($_{4a}$C-$_{5}$C-$_{6}$C-$_{7}$N)	55.68	55.69	53.29	53.23

Fig. 5. Comparison of most stable conformation and the closest one to Aβ fibrils. (A) **14**, (B) **17**, (c) comparison of dihedral angles of two conformations. Closest angles were showed by docking simulation of GOLD. Most stable angles were showed by conformation analysis by SPARTAN′19.

conformation of **17** that interact with the Aβ fibrils. According to the results of previous docking simulations, compounds exhibiting anti Aβ aggregation activity are believed to exerts this effect by forming hydrogen bonds with the hydrophilic part of the Aβ fibril, preventing its aggregation. Therefore, tertiary amine analogues of berberine (**1**) are expected to be potent inhibitors of Aβ aggregation since they can easily change their conformations to interact with Aβ fibril more effectively. To test this hypothesis, we performed docking simulations of Aβ and berberine analogues (Fig. 4) and assessed the structural similarity between the best conformation predicted in the docking simulation and the most stable conformation from the DFT calculations by comparing their dihedral angles. Dihedral angles defined by $_{13}$C-$_{13a}$C-$_{1a}$C-$_{1}$C (a °), $_{13}$C-$_{13a}$C-$_{7}$N−$_{8}$C (b °) and $_{4a}$C-$_{5}$C−$_{6}$C−$_{7}$N (c °) were selected for this evaluation of conformational similarity (Fig. 5). The dihedral angles a ° and b ° in the quaternary ammonium salt **14** were exactly 21.55° and 1.47°, respectively. In addition, angle c ° in **14** differed by only 0.01° (Fig. 5C). For tertiary amine **17** as well, the difference in each

dihedral angle, a °, b ° and c ° was less than 0.1° (Fig. 5D). As a result, it can be concluded that the conformations of **14** and **17** are very similar. On the other hand, dihedral angles b ° of **14** and **17** were 1.47° and 68.0°, respectively – clearly different. Also, the melting point of **14** is higher than that of **17**, reflecting the more efficient packing of the constituent crystals of **14** compared to **17**. However, although **14** and **17** have different properties, their water solubilities and propensity to inhibit the aggregation of Aβ are similar. Interestingly, the length between phenolic hydroxy groups of the **14** and **17** are similar with 3.5 and 2.9 A in spite of the difference configurations of **14** and **17** (Fig. 5C).

3. Conclusion

The total synthesis of berberine (**1**) has been accomplished and its analogues were prepared for the evaluation as Aβ aggregation inhibitors. Berberine (**1**) was found to inhibit moderate Aβ aggregation inhibitory activity and the synthetic intermediates showed no activity, demonstrating the necessity of the berberine framework. Tertiary amine (**17**) bearing four hydroxyl groups was found to have excellent Aβ aggregation inhibitory activity, as well as good water solubility and low cytotoxicity. Further structure activity relationship studies of these berberine analogues are underway in our laboratory.

Author contributions

The manuscript was written through contributions of all authors. All authors have given approval to the final version of the manuscript.

Declaration of competing interest

The authors declare no conflict of interest.

Acknowledgements

This work was supported in part by YU-COE (C) program of Yamagata University.

Appendix A. Supplementary data

Supplementary data to this article can be found online at https://doi.org/10.1016/j.ejmech.2021.113289.

Experimental

General

Solution phase reactions were monitored by thin layer chromatography (Merck Silica gel 60 F_{254}) on glass plates and visualized with *p*-anisaldehyde and heating. Column chromatography was performed using spherical, neutral silica gel of diameter 40–100 μm (Kanto chemical co. Inc., Tokyo, Japan). ^{1}H (400 or 500 or 600 MHz) and ^{13}C NMR (100 or 125 or 150 MHz) spectra were recorded on either a JNM-ECX400 or JNM-ECX500 or JNM-ECZ600 (JEOL, Tokyo, Japan). Chemical shifts are reported in ppm relative to tetramethylsilane (0 ppm), chloroform (7.26 ppm: ^{1}H, 77.1 ppm: ^{13}C), methanol (3.31 ppm: ^{1}H, 49.0 ppm: ^{13}C), and dimethyl sulfoxide (2.50 ppm: ^{1}H, 39.6 ppm: ^{13}C). IR spectra were recorded on a FT/IR-460 Plus (JASCO, Tokyo, Japan). Mass spectra (ESI-MS) were obtained using an AccuTOF JMS-T100LC (JEOL, Tokyo, Japan). High performance liquid chromatography (HPLC) analyses were carried out using a Lachrom ELITE system equipped with a L-2130 pump, a L-2400 UV detector (Hitachi, Tokyo, Japan), and a Cosmosil 5C18-AR-II column (either 4.6 × 150 mm or 10 × 250 mm for preparative work) (Nacalai Tesque, Kyoto, Japan) eluting with a MeCN (0.1% TFA) aqueous solution and detecting at OD 256 nm. Stable conformation analysis was carried out using Wavefunction, Inc, Spartan'18 Parallel Suite for Windows (Irvine, California, USA). The TEM images were obtained with a JSM-7600FA (JEOL, Tokyo, Japan) and an ELS-C10 grid (STEM Cu 100 P specification, pitch 100 μm); electron dying was carried out using 2% tungsten phosphate buffer solution (pH 7.0). Melting points were recorded at on an ATM-02 (AS ONE, Tokyo, Japan) and are uncorrected. Fluorescent microplates were read obtained with a Tecan infinite F200 Pro at an excitation wavelength of 430 nm and a fluorescence wavelength of 485 nm (Tecan, Männedorf, Switzerland). For the cytotoxicity evaluation, a MTP-310 absorbance microplate reader (CORONA, Hitachi-Naka, Japan) was used to measure the absorbance at wavelengths of 450 nm and 630 nm.

1,3-Benzodioxole-5-ethanol (11)

Wittig reagent $[MOMP(Ph)_3]^+$ $[Cl]^-$ (25 g, 73.0 mmol) was suspended in THF (50 mL) under an N_2 atmosphere and *n*-BuLi (25 mL, 299 mmol) was added dropwise at −80 °C. After 30 min, the reaction mixture was warmed to 0 °C. After 90 min, the reaction mixture was cooled to −80 °C. A solution of piperonal (**9**) (5.0 g, 33.0 mmol) in THF (10 mL) was added dropwise and the reaction mixture stirred for 72 h at room temperature. The reaction solution was poured into a saturated ammonium chloride solution. The mixture was added to water and extracted with AcOEt. The obtained organic layer was washed with brine, dried over $MgSO_4$, and concentrated *in vacuo*. The residue was purified with silica gel chromatography using hexane to afford 5-[(1E)-2-methoxyethenyl]-1,3-bendioxisole (4.80 g, 27.0 mmol) as yellow oil. Then, the 5-[(1E)-2-methoxyethenyl]-1,3-bendioxisole was dissolved in acetone (40 mL). 2 M HCl (6 mL) was added to the solution, which was then refluxed for 3 h. Finally, the reaction mixture was added to water and extracted with AcOEt. The obtained organic layers were washed with brine, dried over $MgSO_4$, and concentrated in *vacuo*. The next reaction was carried out immediately without further purification. $NaBH_4$ (1.90 g, 50.2 mmol) was added to the solution of aldehyde (4.1 g, 25 mmol) in MeOH (40 mL) at 0 °C. The reaction mixture was stirred for 4 h, acetone was added, and the mixture stirred for 30 min. The solvent was removed *in vacuo* and the residue was added to water and extracted with AcOEt. The combined organic layers were washed with Brine, dried over $MgSO_4$, and concentrated *in vacuo*. 1,3-Benzodioxole-5-ethanol (**11**) (4.00 g, 73%) was obtained as yellow oil. ^{1}H NMR (600 MHz, $CDCl_3$): δ = 1.40 (brs, 1H), 2.76 (t, *J* = 6.6 Hz, 2H), 3.79 (t, *J* = 6.0 Hz, 2H), 5.92 (s, 2H), 6.66 (dd, *J* = 7.2, 1.2 Hz, 1H), 6.71 (d, *J* = 1.2 Hz, 1H), 6.74 (d, *J* = 7.2 Hz, 1H) ppm. ^{13}C NMR (100 MHz, $CDCl_3$): δ = 38.9, 63.8, 101.0, 108.4, 109.4, 122.0, 132.3, 146.2, 147.8 ppm. IR (film) vmax cm^{-1}: 3358, 2884, 1607, 1503, 1489, 1442, 1361, 1246, 1188, 1099, 1040, 935, 856, 808, 665, 424, 409 cm^{-1}.

5-Bromo-6-(2-bromoethyl)-1,3-benzodioxole (5)

NBS (3.00 g, 16.8 mmol) was added to a solution of **10** (2.32 g, 14.5 mmol) in DMF (10 mL) at 0 °C. The reaction mixture was stirred for 14 h, the mixture was added to water and extracted with AcOEt. The obtained organic layer was washed with brine, dried over $MgSO_4$, and concentrated *in vacuo*. The residue was purified with silica gel chromatography (4:1 = Hexane: AcOEt) to afford 6-bromo-1,3-benzodioxole-5-ethanol (1.60 g, 6.56 mmol) as white crystals. PPh_3 (3.00 g, 11.4 mmol) in THF (15 mL) was added dropwise to a solution of CBr_4 (3.42 g, 10.3 mmol) in THF (10 mL) at 0 °C under an N_2 atmosphere. The reaction mixture was stirred for 1 h. 6-Bromo-1,3-benzodioxole-5-ethanol (1.27 g, 7.65 mmol) in THF

(10 mL) was added and the mixture stirred for 2.5 h. The mixture was added to water and extracted with AcOEt. The combined organic layers were washed with brine, dried over $MgSO_4$, and concentrated *in vacuo*. The residue was purified with silica gel chromatography using hexane to afford 5-bromo-6-(2-bromoethyl)-1,3-benzodioxole (2.58 g, 2 steps 46%) as the oil. ^{1}H NMR (400 MHz, $CDCl_3$): δ = 3.18 (t, *J* = 7.6 Hz, 2H), 3.52 (t, *J* = 7.6 Hz, 2H), 5.96 (s, 2H), 6.74 (s, 1H), 6.99 (s, 1H) ppm. ^{13}C NMR (150 MHz, $CDCl_3$): δ = 31.4, 39.5, 101.9, 110.7, 113.0, 114.6, 131.2, 147.5, 147.6 ppm. IR (film) vmax cm^{-1}: 3072, 3009, 2963, 2895, 2767, 2591, 2309, 2067, 1855, 1700, 1621, 1503, 1476, 1449, 1432, 1408, 1388, 1354, 1313, 1269, 1237, 1168, 1116, 1039, 963, 934, 861, 832, 777, 755, 737, 718, 670, 607, 563, 535,455, 439 cm^{-1}.

2,3-Dimethoxybenzoic acid (7)

Jones reagent (40 mL) was added to a solution of 2,3-dimethoxybenzaldehyde (**6**) (11.0 g, 66.2 mmol) in acetone (50 mL) at 0 °C. The reaction mixture was stirred for 24 h, then added to water and extracted with AcOEt. The obtained organic layer was washed with brine, dried over $MgSO_4$, and concentrated in *vacuo*. 2,3-Dimethoxybenzoic acid (9.60 g, 80%) was obtained as white crystals. Mp: 123–124 °C, ^{1}H NMR (400 MHz, $CDCl_3$): δ = 3.89 (s, 3H), 4.05 (s, 3H), 7.14 (m, 2H), 7.68 (d, *J* = 9.6 Hz, 1H) ppm. ^{13}C NMR (100 MHz, $CDCl_3$): δ = 56.2, 62.1, 117.5, 122.5, 123.7, 124.9, 148.5, 152.4, 166.6 ppm. IR (film) vmax cm^{-1}: 2941, 1698, 1579, 1483, 1423, 1320, 1267, 1231, 1053, 1001, 938, 820, 806, 757, 730, 665, 425, 409 cm^{-1}. ESIHRMS *m/z*: calcd. for $C_9H_{10}NaO_4$ $[M+Na]^+$ 205.0477, found: 205.0455.

N -(2,2-diethoxyethyl)-2,3-dimethoxy-benzamide (8)

$SOCl_2$ (12 mL, 164 mmol) was added to a solution of **7** (7.40 g, 40.6 mmol) in CH_2Cl_2 (30 mL) at −80 °C. The reaction mixture was stirred for 20 h at room temperature. After confirming the disappearance of 2,3-dimethoxybenzoic acid (by TLC), the solvent was removed in *vacuo*. The mixture was dissolved in THF (50 mL). Then, DIPEA (14.0 mL, 80.4 mmol) and aminoacetaldehyde diethyl acetal (13.0 mL, 89.8 mmol) were added to the solution at 0 °C. The mixture was stirred for 24 h. After the reaction, the mixture was added to water and extracted with AcOEt. The obtained organic layer was washed with brine, dried over $MgSO_4$, and concentrated in *vacuo*. The residue was purified with silica gel chromatography (4 : 1 = hexane: AcOEt) to afford *N*-(2,2-diethoxyethyl)-2,3-dimethoxy-benzamide (**8**) (10.0 g, 83%) as yellow oil. ^{1}H NMR (600 MHz, $CDCl_3$): δ = 1.00 (t, *J* = 7.2 Hz, 6H), 3.35 (m, 4H), 3.49 (m, 2H), 3.62 (s, 3H), 3.66 (s, 3H), 4.40 (t, *J* = 5.4 Hz, 1H), 6.86 (dd, *J* = 9.0, 1.6 Hz, 1H), 6.68 (t, *J* = 9.0 Hz, 1H), 7.42 (d, *J* = 1.6 Hz, 1H), 8.09 (brs, 1H) ppm. ^{13}C NMR (100 MHz, $CDCl_3$): δ = 15.2, 42.0, 55.9, 61.1, 62.3, 100.6, 115.3, 122.5, 124.1, 126.3, 147.6, 152.5, 165.0 ppm. IR (film) vmax cm^{-1}: 3381, 3077, 2975, 1971, 1732, 1659, 1578, 1530, 1474, 1375, 754, 438 cm^{-1}. ESIHRMS *m/z*: calcd. for $C_{15}H_{23}NNaO_5$ $[M+Na]^+$ 320.1474, found: 320.1452.

7,8-Dimethoxy-1 (2H) –isoquinolinone (4)

Conc. H_2SO_4 (20 mL) was added dropwise to solid **8** (15.6 g, 52.4 mmol) at 0 °C. The reaction mixture was stirred for 72 h. Then, 2 M NaOH (40 mL) was added. The mixture was added to water and extracted with CH_2Cl_2. The obtained organic layer was washed with brine, dried over $MgSO_4$, and concentrated in *vacuo*. The residue was purified with silica gel chromatography (95 : 5 = Chloroform: MeOH) to afford 7,8-Dimethoxy-1 (2*H*) -isoquinolinone (**4**) (8.30 g, 77%) as light yellow crystals. Mp:182–184 °C, ^{1}H NMR (400 MHz, $CDCl_3$): δ = 3.85 (s, 3H), 3.97 (s, 3H), 6.31 (d, *J* = 7.2 Hz, 1H), 7.05 (d, *J* = 7.2 Hz, 1H), 7.26 (m, 2H), 11.33 (brs, 1H) ppm. ^{13}C NMR (100 MHz, $CDCl_3$): δ = 57.0, 62.0, 106.1, 119.4, 121.0, 122.4, 126.3, 134.0, 149.7, 151.5, 162.9 ppm. IR (film) vmax cm^{-1}: 3583, 1637, 1493, 1279, 1226, 1071, 1046, 827, 665, 655, 408 cm^{-1}. ESIHRMS *m/z*: calcd. for $C_{11}H_{11}NNaO_3$ $[M+Na]^+$ 228.0637, found: 228.0666.

2-[(6-Bromo-1,3-benzodioxol-5-yl) ethyl]-7,8-dimethoxy-1(2H)-isoquinolinone (3)

Cs_2CO_3 (160 mg, 0.491 mmol) and **5** (93.6 mg, 0.306 mmol) were added to a solution of **4** (50.0 mg, 0.244 mmol) in DMF (5 mL). The reaction mixture was heated to 80 °C and stirred for 8 h. The mixture was added to water and extracted with AcOEt. The obtained organic layer was washed with brine, dried over $MgSO_4$, and concentrated *in vacuo*. The residue was purified with silica gel chromatography (4 : 1 = hexaxe: AcOEt) to afford 2-[(6-Bromo-1,3-benzodioxol-5-yl)ethyl]-7,8-dimethoxy-1(2*H*)-isoquinolinone (**3**) (34.0 mg, 32%) as white-yellow crystals. Mp: 174–176 °C, ^{1}H NMR (400 MHz, $CDCl_3$): δ = 3.10 (t, *J* = 7.2 Hz, 2H), 3.91 (s, 3H), 3.97 (s, 3H), 4.06 (t, *J* = 7.6 Hz, 2H), 5.91 (s, 2H), 6.25 (d, *J* = 7.6 Hz, 1H), 6.72 (m, 2H), 7.17 (s, 1H), 7.18 (d, *J* = 8.8 Hz, 1H), 7.26 (m, 1H) ppm. ^{13}C NMR (100 MHz, $CDCl_3$): δ = 35.3, 49.6, 57.0, 61.7, 101.8, 105.4, 111.0, 112.8, 114.7, 118.9, 121.0, 122.1, 130.2, 130.8, 133.0, 147.4, 147.6, 149.8, 151.8, 160.2 ppm. IR (film) vmax cm^{-1}: 2930, 1653, 1622, 1497, 1477, 1422, 1369, 1280, 1231, 1132, 1073, 1037, 987, 932, 824, 754, 666, 406 cm^{-1}. ESIHRMS *m/z*: calcd. for $C_{20}H_{18}BrNO_5$ [M] 432.0425, found: 432.0425.

5,6-dihydro-9,10-dimethoxy-8H-benzo[g]-1,3-benzodioxolo[5,6-a] quinolizin-8-one (2)

DIPEA (0.1 mL, 0.574 mmol) and PPh_3 (51.0 mg, 19.4 μmol) were added to the solution of **3** (20 mg, 46.3 μmol) in toluene (8 mL). After $Pd(OAc)_2$ (11.0 mg, 49.0 μmol) was added, the mixture was stirred for 24 h at 80 °C under an N_2 atmosphere. The mixture was filtered through a celite pad, the filtrate added to water and then extracted with AcOEt. The obtained organic layer was washed with brine, dried over $MgSO_4$, and concentrated in *vacuo*. The residue was purified with silica gel chromatography (2 : 1 = hexane: AcOEt) to afford 5,6-dihydro-9,10-dimethoxy-8*H*-benzo[*g*]-1,3-benzodioxolo[5,6-*a*]quinolizin-8-one (4.0 mg, 25%) as yellow crystals. Mp: 198–200 °C, ^{1}H NMR (400 MHz, $CDCl_3$): δ = 2.92 (t, *J* = 7.2 Hz, 2H), 3.96 (s, 3H), 4.04 (s, 3H), 4.32 (t, *J* = 7.6 Hz, 2H), 6.04 (s, 2H), 6.62 (s, 1H), 6.75 (s, 1H), 7.24 (s,1H), 7.31 (m, 2H) ppm. ^{13}C NMR (100 MHz, $CDCl_3$): δ = 28.8, 39.5, 56.9, 61.7, 101.4, 101.5, 104.8, 108.0, 118.9, 119.4, 122.4, 123.8, 130.1, 132.3, 135.7, 147.4, 148.5, 149.5, 151.5, 160.2 ppm. IR (film) vmax cm^{-1}: 2927, 1718, 1649, 1617, 1596, 1493, 1382, 1278, 1226, 1174, 1099, 1084, 1037, 937, 868, 804, 753, 695, 665, 421 cm^{-1}. ESIHRMS *m/z*: calcd. for $C_{20}H_{18}NO_5$ $[M+H]^+$ 352.1185; found: 352.1210.

Berberine (1)

$LiAlH_4$ (80.0 mg, 21.1 mmol) was added to a solution of **2** (100 mg, 0.285 mmol) in THF (10 mL). The mixture was refluxed with stirring for 2 h. Then, H_2O (0.26 mL) and NaOH (0.13 mL) were added and the mixture stirred for an additional 30 min. $KHSO_4$ aq. (20 mL) was added and the mixture stirred for another 1 h. The mixture was added to water and extracted with CH_2Cl_2. The obtained organic layer was washed with brine, dried over $MgSO_4$, and concentrated *in vacuo*. The residue was purified with silica gel chromatography (90 : 10 = chloroform: MeOH) to afford berberine (**1**) (15.0 mg, 44.6 μmol, 16%) as yellow crystals. Mp:208–210 °C, ^{1}H NMR (600 MHz, DMSO-d_6): δ = 3.18 (t, *J* = 6.0 Hz, 2H), 4.06 (s, 3H), 4.08 (s, 3H), 4.91 (t, *J* = 6.0 Hz, 2H), 6.17 (s, 2H), 7.08 (s, 1H), 7.79 (s, 1H), 7.98 (d, *J* = 9.0 Hz, 1H),8.19 (d, *J* = 9.0 Hz, 1H), 8.92 (s, 1H), 9.88 (s, 1H) ppm. IR (film) vmax cm^{-1}: 2922, 2851, 1669, 1507, 1457, 1436, 1387, 1363, 1274, 1174, 1131, 1042, 771, 724, 698, 665, 455, 440, 425, 409 cm^{-1}. ESIHRMS *m/z*: calcd. for $C_{20}H_{18}ClNO_4$ $[M\text{-}Cl^-]^+$ 336.1235, found: 336.1204.

2,3-Dihydroxy-9,10-dimethoxy-5,6-dihydroisoquinolino[3,2-a] isoquinolinium (12)

9-Methoxy-2,3,10-trihydroxy-5,6-dihydroisoquinolino[3,2-a] isoquinolinium (13)

Boron tribromide (2 mL) was added dropwise to the solution of Berberine (500 mg, 1.49 mmol) in dry dichloromethane (7 mL) at −80 °C. The mixture was stirred for 30 min. The mixture was slowly heated to 30 °C and stirred for 18.5 h, water was added and the solvent removed *in vacuo*. The residue was purified by silica gel chromatography (90 : 10 = chloroform: MeOH) to afford 2,3-dihydroxy-9,10-dimethoxy-5,6-dihydroisoquinolino[3,2-a]isoquinolinium (**12**) (68 mg, 13%) as yellow powder and 9-methoxy-2,3,10-trihydroxy-5,6-dihydroisoquinolino[3,2-a]isoquinolinium (**13**) (4.33 mg, 1%) as red solid. **12**: Mp 164–165 °C, ^{1}H NMR (600 MHz, DMSO-d_6): δ = 3.06 (t, *J* = 6.0 Hz, 2H), 4.02 (s, 3H), 4.04 (s, 3H), 4.84 (t, *J* = 6.0 Hz, 2H), 6.77 (s, 1H), 7.46 (s, 1H), 8.00 (d, *J* = 9.0 Hz, 1H), 8.13 (d, *J* = 9.0 Hz, 1H), 8.72 (s, 1H), 9.29 (brs, 1H), 9.80 (s, 1H), 10.07 (brs, 1H) ppm. ^{13}C NMR (150 MHz, DMSO-d_6): δ = 26.2, 56.1, 57.6, 62.4, 113.2, 115.4, 118.3, 119.6, 121.7, 124.1, 127.2, 127.7, 133.8, 144.0, 145.7, 146.1, 149.7, 150.5 ppm. IR (film) vmax cm^{-1}: 3421, 1608, 1561, 1531, 1457, 1365, 1333, 1262, 1141, 1107, 1065, 999, 979, 901, 869, 826, 505, 425, 415 cm^{-1}.ESIHRMS *m/z*: calcd. for $C_{19}H_{18}ClNO_4$ [M-Cl$^-$]$^+$ 324.1230, found: 324.1206.**13**: Mp: 178–179 °C, ^{1}H NMR (500 MHz, MeOH-d_4): δ = 3.03 (t, *J* = 6.0 Hz, 2H), 3.98 (s, 3H), 4.80 (t, *J* = 6.6 Hz, 2H), 6.75 (s, 1H), 7.44 (s, 1H), 7.69 (d, *J* = 9.0 Hz, 1H), 8.01 (d, *J* = 9.0 Hz, 1H), 8.61 (s, 1H), 9.26 (s, 1H), 9.81 (s, 1H), 10.03 (s, 1H), 11.14 (s, 1H) ppm. ^{13}C NMR (150 MHz, MeOH-d_4): δ = 26.7, 55.9, 55.9, 111.8, 114.4, 114.4, 118.0, 118.5, 119.0, 127.1, 128.8, 137.4, 142.1, 143.5, 144.1, 145.7, 149.0, 149.1 ppm. IR (film) vmax cm^{-1}: 3178, 1609, 1509, 1458, 1308, 875, 428, 412 cm^{-1}. ESIHRMS *m/z*: calcd. for $C_{19}H_{16}ClNO_4$ [M-Cl$^-$]$^+$ 310.1074, found: 310.1006.

2,3,9,10-Tetrahydroxy-5,6-dihydroisoquinolino[3,2-a] isoquinolinium (14)

Boron tribromide (3 mL) was added dropwise to a solution of berberine (**1**) (400 mg, 1.19 mmol) in dry dichloromethane (6 mL) at 0 °C. The mixture was slowly warmed to room temperature and stirred. After 14.5 h, water was added to the mixture and the solvent removed in *vacuo*. The residue was purified with column chromatography (90 : 10 = chloroform: MeOH) to afford 2,3,9,10-Tetrahydroxy-5,6-dihydroisoquinolino[3,2-a]isoquinolinium (**14**) (130 mg, 37%) as brown crystal. Mp: 186–187 °C, ^{1}H NMR (600 MHz, DMSO-d_6): δ = 3.03 (t, *J* = 6.0 Hz, 2H), 4.78 (t, *J* = 6.0 Hz, 2H), 6.75 (s, 1H), 7.44 (s, 1H), 7.58 (d, *J* = 9.0 Hz, 1H), 7.72 (d, *J* = 9.0 Hz, 1H), 8.56 (s, 1H), 9.23 (s, 1H), 9.71 (s, 1H), 9.99 (s, 1H) 10.64 (s, 1H), 10.72 (s, 1H) ppm. ^{13}C NMR (150 MHz, DMSO-d_6): δ = 26.4, 55.7, 113.0, 115.4, 118.6, 118.6, 118.7, 119.3, 127.4, 129.5, 132.8, 137.2, 141.7, 143.8, 145.0, 145.9, 149.2 ppm. IR (film) vmax cm^{-1}: 3606, 2860, 1656, 1576, 1409, 1340, 1253, 1137, 1044, 1025, 951, 845, 762 cm^{-1}. ESIHRMS *m/z*: calcd. for $C_{17}H_{14}ClNO_4$ [M-Cl$^-$]$^+$ 296.0917, found: 296.0933.

5,6,13,13a-tetrahydro-9,10-dimethoxy-2,3-(methylenedioxy)-8H-dibenzo[a,g] quinolizine (15)

$NaBH_4$ (200 mg, 5.29 mmol) was added to a solution of Berberine (**1**) (500 mg, 1.50 mmol) in MeOH (30 mL) at 0 °C. The reaction mixture was stirred for 17 h at room temperature. Then, the MeOH was removed *in vacuo*. The mixture was added to water and extracted with chloroform/MeOH (95 : 5). The obtained organic layer was washed with brine, dried over $MgSO_4$, and concentrated *in vacuo*. 5,6,13,13a-Tetrahydro-9,10-dimethoxy-2,3-(methylenedioxy)-8H-dibenzo[a,g]quinolizine (**15**) (377 mg, 83%) was obtained as light yellow crystals without further purification. Mp:163–165 °C, ^{1}H NMR (500 MHz, $CDCl_3$): δ = 2.60 (dd, *J* = 16.0, 3.5 Hz, 1H), 2.64 (d, *J* = 16.0 Hz, 1H), 2.78 (d, *J* = 16.0 Hz, 1H), 3.08 (m, 2H), 3.20 (dd, *J* = 16.0, 4.0 Hz, 1H), 3.51 (d, *J* = 16.0 Hz, 2H), 3.84 (s, 6H), 4.21 (d, *J* = 16.0 Hz, 1H), 5.91 (s, 2H), 6.59 (s, 1H), 6.73 (s, 1H), 6.77 (d, *J* = 8.5 Hz, 1H), 6.85 (d, *J* = 8.5 Hz, 1H) ppm. ^{13}C NMR (150 MHz, $CDCl_3$): δ = 29.7, 36.6, 51.5, 54.0, 56.0, 59.8, 60.3, 100.9, 105.6, 108.5, 111.0, 124.0, 127.9, 128.8, 130.9, 145.1, 146.0, 146.2, 150.4 ppm. IR (film) vmax cm^{-1}:2952, 2860, 2777, 1525, 1389, 1334, 1304, 1248, 1160, 1038, 1015, 990, 956, 845, 805 cm^{-1}. ESIHRMS *m/z*: calcd. for $C_{20}H_{22}NO_4$ [M+H]$^+$ 340.1549, found: 340.1571.

5,6,13,13a-tetrahydro-9-methoxy-2,3,10-trihydroxy-8H-dibenzo [a,g]quinolizine (16)

Boron tribromide (600 μL) was added dropwise to a solution of **15** (204 mg, 601 μmol) in dry dichloromethane (2 mL) at −80 °C. The mixture was stirred for 10 min. Then the mixture was slowly heated to 0 °C and stirred for 15 h. After the reaction, water was added to the mixture and solvent was removed *in vacuo*. The residue was purified by silica gel chromatography (90 : 10 = chloroform: MeOH) to afford 5,6,13,13a-Tetrahydro-9-methoxy-2,3,10-trihydroxy-8H-dibenzo[a,g]quinolizine (**16**) (82.3 mg, 44%) as orange crystals. Mp: 175–176 °C, ^{1}H NMR (600 MHz, MeOH-d_4): δ = 2.90 (d, *J* = 15.0 Hz, 1H), 2.97 (q, *J* = 11.4 Hz, 1H), 3.18 (td, *J* = 13.2, 4.2 Hz, 1H), 3.50 (t, *J* = 12.0 Hz, 1H), 3.63 (m, 1H), 3.82 (m, 4H), 4.28 (dd, *J* = 15.0, 5.4 Hz, 1H), 4.63 (td, *J* = 12.0, 4.2 Hz, 1H), 4.70 (m, 1H), 6.62 (s, 1H), 6.64 (d, *J* = 8.4 Hz, 1H), 6.76 (m, 2H) ppm. ^{13}C NMR (150 MHz, DMSO-d_6): δ = 25.3, 32.9, 50.8, 51.6, 56.6, 59.4, 112.2, 112.8, 115.5, 119.4, 119.5, 122.6, 123.0, 124.9, 142.7, 145.1, 145.7, 146.2 ppm. IR (film) vmax cm^{-1}: 3394, 1607, 1497, 1457, 1363, 1278, 1053, 867, 749, 471 cm^{-1}. ESIHRMS *m/z*: calcd. for $C_{18}H_{20}NO_4$ [M+H]$^+$ 314.1392, found: 314.1393.

5,6,13,13a-tetrahydro-2,3,9,10-tetrahydroxy-8H-dibenzo[a,g] quinolizine (17)

Boron tribromide (1.2 mL) was added dropwise to a solution of **15** (100 mg, 295 μmol) in dry dichloromethane (3 mL) at −80 °C. The mixture was slowly heated to room temperature and stirred for 11 h; water was added, and solvent was removed *in vacuo*. The residue was purified by silica gel chromatography (90 : 10 = chloroform: MeOH) to afford 5,6,13,13a-Tetrahydro-2,3,9,10-tetrahydroxy-8H-dibenzo[a,g]quinolizine (**17**) (24.7 mg, 28%) as light yellow crystals. Mp 201–203 °C, ^{1}H NMR (600 MHz, MeOH-d_4): δ = 2.91 (dd, *J* = 16.2, 2.4 Hz, 1H), 2.98 (m, 1H), 3.17 (td, *J* = 12.6, 4.8 Hz, 1H), 3.50 (td, *J* = 12.6, 4.2 Hz, 1H), 3.65 (d, *J* = 17.4, 4.2 Hz, 1H), 3.86 (dd, *J* = 11.4, 4.8 Hz, 1H), 4.30 (d, *J* = 15.0 Hz, 1H), 4.65 (dd, *J* = 12.0, 4.2 Hz, 1H), 4.72 (d, *J* = 16.2 Hz, 1H), 6.64 (s, 1H), 6.66 (d, *J* = 7.2 Hz, 1H), 6.77 (d, *J* = 7.2 Hz, 1H), 6.80 (s, 1H) ppm. ^{13}C NMR (150 MHz, DMSO-d_6): δ = 25.4, 33.0, 49.1, 50.9, 59.5, 112.8, 115.5, 115.6, 116.8, 119.5, 122.5, 123.0, 123.1, 141.9, 143.7, 145.2, 145.7 ppm. IR (film) vmax cm^{-1}: 3652, 3550, 3268, 1656, 1554, 1522, 1335, 1304, 1132, 1011, 909, 826, 762, 678 cm^{-1}. ESIHRMS *m/z*: calcd. for $C_{17}H_{18}NO_4$ [M+H]$^+$ 300.1236, found: 300.1227.

Assay of aβ aggregation inhibitory activity

The aggregation of Aβ was assessed with the ThT method. Briefly, 25 μM Aβ42 (Peptide Institute, Inc.; Ibaraki, Japan) was combined with 0 μM (control) or 10 μM BBR intermediates or analogues in the presence of 50 mM sodium phosphate buffer, pH 7.5, 100 mM NaCl, 1% (v/v) DMSO. The total fluid volume was 25 μL. Reactions were incubated at 37 °C. To monitor amount of Aβ aggregate, aliquots were diluted fourfold into 5 μM ThT and immediately evaluated for fluorescence (excitation = 445 nm, emission = 490 nm).

Docking simulation

The 3D coordinates of Aβ fibrils were obtained from the Protein data bank (PDB ID: 2MXU). The ligand was docked into the binding sites of Aβ fibrils as assigned to CA Phe-20 (20 Å) by GOLD software and visualized by PyMOL software.

Transmission electron microscopy (TEM) experiments

Carbon-coated copper grid was overlaid with a suspension of Aβ fibrils and then blotted dry with a filter paper. The grids were washed, negatively stained with 1% phosphotungstate acid and dried in air before being examined in a JEM-2100 transmission electron microscope at an accelerating voltage of 200 kV.

DLS measurement

Aβ solution (25 μM Aβ, 5 mM sodium phosphate buffer, pH 7.5, 10 mM NaCl, 0.1% (v/v) DMSO) was prepared as previously described and extruded through a polycarbonate membrane with a pore size of 200 nm (Sartorius, Germany) using a Minisart syringe filter (Sartorius). Dynamic light scattering measurements were performed immediately after preparation and after 20 h to track to oligomer size over time. DLS measurements were performed using a Malvern Zetasizer with a glass cuvette.

Aqueous solubility test

The aqueous solubility of the compounds was ascertained using the shake flask method. Briefly, about 1 mg of compound was dispersed in 1.0 mL of water. The suspension was shaken for 12 h at 37 °C. An aliquot was filtered through a Millipore Cosmospin Filter H (0.45 μm). The filtrate was diluted in MeOH or DMSO and injected into an HPLC with UV detection; peak heights were recorded at 256 nm. The concentration of the sample solution was calculated using a previously determined calibration curve, corrected for the dilution factor of the sample.

Evaluation of the cytotoxicity by MTT assay

PC12 cells were maintained in a suspension culture of DMEM supplemented with 5% FBS (Fetal Bovine Serum) containing 1% of a penicillin-streptomycin (1:1) mixture. A 100 μL aliquot of PC12 cells (10,000 cells/mL) was added to a 96 well plate and incubated for 24 h at 37 °C in a humidified incubator containing 5% CO_2 in air. After 24 h, a 10 μL aliquot of compound BBR analogues (concentrations varying in the range of 10–150 μM) was added to each of the 96 wells and incubated for 24 h. A 10 μL WST-8 solution (mixture of WST-8 and 1-Methoxy PMS) was added to each well and the incubation continued for 3 h. The visible absorbance at 450 nm and 630 nm as the reference wavelength of each well was quantified using a microplate reader.

References

[1] D.M. Walsh, D.J. Selkoe, A beta oligomers- a decade of discovery, J. Neurochem. 101 (2007) 1172–1184.

[2] M. Hashimoto, E. Rockenstein, L. Crews, E. Masliah, Role of protein aggregation in mitochondrial dysfunction and neurodegeneration in Alzheimer's and Parkinson's diseases, Neuromol. Med. 4 (2003) 21–35.

[3] S. Shishodia, M.M. Chaturvedi, B.B. Aggrwal, Role of curcumin in cancer therapy, Curr. Probl. Canc. 31 (2007) 243–305.

[4] H. Ohtsu, Z. Xiao, J. Ishida, M. Nagai, H.-K. Wang, H. Itokawa, C.-H. Su, C. Shih, T. Chiang, E. Chang, Y. Lee, M.-Y. Tsai, C. Chang, k.-H. Lee, Antitumor agents. 217. Curcumin analogues as novel androgen receptor antagonists with potential as anti-prostate cancer agents, J. Med. Chem. 45 (2002) 5037–5042.

[5] T. Hamaguchi, K. Ono, A. Murase, M. Yamada, Phenolic compounds prevent Alzheimer's pathology through different effects on the amyloid-beta aggregation pathway, Am. J. Pathol. 175 (2009) 2557–2565.

[6] A.N. Begum, M.R. Jones, G.P. Lim, T. Morihara, P. Kim, D.D. Heath, C.L. Rock, M.A. Pruitt, F. Yang, B. Hudspeth, S. Hu, K.F. Faull, B. Teter, G.M. Cole, S.A. Frautschy, Curcumin structure-function, bioavailability, and efficacy in models of neuroinflammation and Alzheimer's disease, J. Pharmacol. Exp. Therapeut. 326 (2008) 196–208.

[7] J.M. Ringman, S.A. Frautschy, E. Teng, A.N. Begum, J. Bardens, M. Beigi, K.H. Gylys, V. Badmaev, D.D. Heath, L.G. Apostolova, V. Porter, Z. Vanek, G.A. Marshall, G. Hellemann, C. Sugar, D.L. Masterman, T.J. Montine, J.L. Cummings, G.M. Cole, Oral curcumin for Alzheimer's disease: tolerability and efficacy in a 24-week randomized, double blind, placebo-controlled study, Alzheimers Reseach & Therapy 4 (2012) 43.

[8] P. Anand, A.B. Kunnumakkara, R.A. Newman, B.B. Aggarwal, Bioavailability of curcumin: problems and promises, Mol. Pharm. 4 (2007) 807–818.

[9] M. Hotsumi, M. Tajiri, K. Makabe, H. Konno, Design, synthesis and evaluation of diaryl γ-dihydropyrone dirivatives as cyclocurcumin mimetics and inhibitors of the aggeragation of amyloid β, Bioorg. Chem. 104 (2020) 104302.

[10] M. Hotsumi, M. Tajiri, Y. Nikaido, T. Sato, K. Makabe, H. Konno, Design, synthesis, and evaluation of a water soluble C5-monoketone type curcumin analogue as a potent amyloid β aggregation inhibitor, Bioorg. Med. Chem. Lett 29 (2019) 2157–2161.

[11] T. Sato, M. Hotsumi, K. Makabe, H. Konno, Design, synthesis and evaluation of curcumin-based fluorescent probes to detect Aβ fibrils, Bioorg. Med. Chem. Lett 28 (2018) 3520–3525.

[12] H. Endo, Y. Nikaido, M. Nakadate, S. Ise, H. Konno, Structure activity relationship study of curcumin analogues toward the amyloid-beta aggregation inhibitor, Bioorg. Med. Chem. Lett 24 (2014) 5621–5626.

[13] H. Konno, H. Endo, S. Ise, K. Miyazaki, H. Aoki, A. Sanjoh, K. Kobayashi, Y. Hattori, K. Akaji, Synthesis and evaluation of curcumin derivatives toward an inhibitor of beta-site amyloid precursor protein cleaving enzyme 1, Bioorg. Med. Chem. Lett. 24 (2014) 685–690.

[14] B. Matharu, G. Gibson, R. Parsons, T.N. Huckerby, S.A. Moore, L.J. Cooper, R. Millichamp, D. Allsop, B. Austen, Galantamine inhibits beta-amyloid aggregation and cytotoxicity, J. Neurol. Sci. 280 (2009) 49–58.

[15] Q. Sun, F. Liu, J. Sang, M. Lin, J. Ma, X. Xiao, S. Yan, C.B. Naman, N. Wang, S. He, X. Yan, W. Cui, H. Liang, 9-Methylfascaplysin is a more potent Aβ aggregation inhibitor than the marine-derived alkaloid, fascaplysin and produces nanomolar nuoroprotective effects in SH-SY5Y cells, Mar. Drugs 17 (2019) 121–136.

[16] C.-L. Kuo, C.-W. Chi, T.-Y. Liu, The anti-inflammatory potential of berberine in vitro and in vivo, Canc. Lett. 203 (2004) 127–137.

[17] F.R. Stermitz, P. Lorenz, J.N. Tawara, L.A. Zenewicz, K. Lewis, Synergy in a medicinal plant: antimicrobial action of berberine potentiated by 5'-methoxyhydnocarpin, a multidrug pump inhibitor, Proc. Natl. Acad. Sci. U.S.A. 97 (2000) 1433–1437.

[18] M.L. Aski, M.E. Rezvani, M. Khaksari, Z. Hafizi, Z. Pirmoradi, S. Niknazar, F.Z. Mehrjerdi, Neuroprotective effect of berberine chloride on cognitive impairment and hippocampal damage in experimental model of vascular dementia, Iran, J. Basic. Med. Sci. 21 (2018) 53–58.

[19] J. Zhang, J.-Q. Yang, B.-C. He, Q.-X. Zhou, H.-R. Yu, Y. Tang, B.-Z. Liu, Berberine and total base from rhizoma coptis chinensis attenuate brain injury in an aluminum-induced rat model of neurodegenerative disease, Saudi Med. J. 30 (2009) 760–766.

[20] L.M. Mori-Quiroz, S.L. Hedrick, A.R. De Los Santos, M.D. Clift, A unified strategy for the synthesis alkaloids berberine, coptisine, and jatrorrhizine, Org. Lett. 20 (2018) 4281–4284.

[21] G. Lahm, J.-G. Deichmann, A.L. Rauen, T. Opatz, A one-pot cascade to protoberberine alkaloids via Stevens rearrangement of nitrile-stabilized ammonium ylides, J. Org. Chem. 80 (2015) 2010–2016.

[22] S. Zhou, R. Tong, A genetal, concise strategy that enables collective total syntheses of over 50 protoberberine and five aporhoeadane alkaloids within four to eight steps, Chem. Eur J. 22 (2016) 7084–7089.

[23] Y. He, Y. Zheng, L. Hai, Y. Wu, A versatile total synthesis of 8-oxyberberine and oxohomoberberines, chin, J. Chem. 32 (2014) 1121–1127.

[24] A.C. Shaikh, D.R. Shinde, N.T. Patil, Gold vs rhodium catalysis: tuning reactivity through catalyst control in the C-H alkynylation of isoquinolones, Org. Lett. 18 (2016) 1056–1059.

[25] S. Namioka, N. Yoshida, H. Konno, K. Makabe, Residue-specific binding mechanisms of Thioflavin T to a surface of flat β-sheets within a peptide self-assembly mimic, Biochemistry 59 (2020) 2782–2787.

[26] M.E. Abouelela, M.A.A. Orabi, R.A. Abdelhamid, M.S.A. Abdelkader, F.M.M. Darwish, M. Hotsumi, H. Konno, Anti-Alzheimer's flavanolignans from *Ceiba pentandra* aerial parts, Fitoterapia 143 (2020) 104541.

[27] A. Tan, R. Suzuki, C. Yokoyama, S. Yano, H. Konno, Antimicrobial activity and secondary structure of a novel peptide derived from ovalbumin, J. Pept. Sci. 26 (2020), e3276.

[28] M. Nakano, M. Fukuda, T. Kudo, N. Matsuzaki, T. Azuma, K. Sekine, H. Endo, T. Handa, Flip-flop of phospholipids in vesicles: kinetic analysis with time-resolved small-angle neutron scattering, J. Phys. Chem. B 119 (2009) 6745–6748.

[29] H.L. 3rd, Thioflavine T interaction with synthetic Alzheimer's disease beta-amyloid peptides: detection of amyloid aggregation in solution, Protein Sci. 2 (1993) 404–410.

[30] R. Sato, K. Oyama, H. Konno, Investigation for the cyclization efficiency of linear tetrapeptides: synthesis of tentoxin B and dihydrotentoxin,

Tetrahedron 74 (2018) 6173–6181.
[31] M. Kikuchi, H. Konno, Cytotoxic evaluation of natural and synthetic callipeltins: a revision of cytotoxicity of callipeltin B, Biosci. Biotechnol. Biochem. 80 (2016) 1066–1069.
[32] S. Dorai, W. Shi, C. Corbo, C. Sun, S. Averick, D. Obeysekera, M. Farid, A. Alonso, P. Banerjee, K. Raja, "Clicked" sugar-curcumin conjugate: modulator of amyloid-β and tau peptide aggregation at ultralow concentrations, ACS Chem. Neurosci. 2 (2011) 694–699.
[33] M. Ishiyama, Y. Miyazono, K. Sasamoto, Y. Ohkura, K. Ueno, A highly water-soluble disulfonated tetrazolium salt as a chromogenic indicator for NADH as well as cell viability, Talanta 44 (1997) 1299–1305.
[34] S.A. Hitchcock, L.D. Pennington, Structure-brain exposure relationships, J. Med. Chem. 49 (2006) 7559–7583.
[35] C.A. Lipinski, F. Lombardo, B.W. Dominy, P.J. Feeney, Experimental and computational approaches to estimate solubility and permeability in drug discovery and development settings, Adv. Drug Deliv. Rev. 23 (1997) 3–26.
[36] Q. Zhang, J. Liu, X. Hu, W. Wang, Z. Yuan, In vitro studies on accelerating the degradation and clearance of amyloid-β fibrils by an antiamyloidogenic peptide, ACS Macro Lett. 4 (2015) 339–342.
[37] V.L. Anderson, T.F. Ramlall, C.C. Rospiglioating the, W.W. Webb, D. Eliezer, Identification of a helical intermediate in trifluoroethanol-induced alpha-synuclein aggregation, PNAS 107 (2010) 18850–18855.
[38] The software was prepared by the Cambridge Crystallographic Data Centre (CCDC). http://www.ccdc.cam.ac.uk.
[39] Inc The software was prepared by Wavefunction. http://www.wavefun.com.